

Proteome-level changes in two *Brassica napus* lines exhibiting differential responses to the fungal pathogen *Alternaria brassicae*

Nidhi Sharma, Muhammad Hafizur Rahman, Stephen Strelkov, Mohan Thiagarajah, Vipin K. Bansal¹, Nat N.V. Kav^{*}

Department of Agricultural, Food and Nutritional Science, University of Alberta, Edmonton, Alberta T6G 2P5, Canada

Received 13 June 2006; received in revised form 21 July 2006; accepted 24 July 2006

Available online 15 August 2006

Abstract

Two *Brassica* lines derived from an interspecific cross between *Brassica napus* and *B. carinata* were evaluated for tolerance to the fungal pathogen *Alternaria brassicae*. Pathogen-induced chlorosis and necrosis spread significantly in one line whereas it remained localized in the other. Proteome-level changes in response to the fungal pathogen were investigated using two-dimensional electrophoresis. Levels of 48 proteins were significantly affected at various time points in the tolerant line (41 up-regulated and 7 down-regulated). In contrast, in the susceptible line, we observed the levels of 23 proteins to be significantly affected with 4 increasing and 19 decreasing. We were successful in establishing the identities of 38 proteins and those identified from the tolerant line included enzymes involved in the generation of reactive oxygen species (ROS), ROS mediated signaling, auxin signal transduction and metabolic pathways. Proteome-level results suggesting a role for ROS mediated auxin signaling in this pathosystem was further investigated and confirmed using quantitative real-time PCR. Our findings are discussed within the context of *A. brassicae*–*B. napus* interaction and, tolerance to this pathogen.

© 2006 Elsevier Ireland Ltd. All rights reserved.

Keywords: *Alternaria brassicae*; Canola (*Brassica napus*); Mass spectrometry; Proteomics; Two-dimensional gel electrophoresis

1. Introduction

Canola (*Brassica napus*) is a major crop cultivated in Western Canada and among the various factors limiting canola productivity is the disease Alternaria blackspot, caused by the fungal pathogen *Alternaria brassicae*. This pathogen is one of the most destructive diseases affecting *B. napus*, *B. rapa* and *B. juncea* and outbreaks of Alternaria blackspot can result in yield reductions of up to 36% [1–4]. *A. brassicae* can infect virtually any part of the plant and visible symptoms of infection include chlorotic and necrotic lesions on the leaf, petiole, stem, inflorescence, silique and seed [1]. Generally, yield reductions as a result of *A. brassicae* infection are the result of infected siliques which lead to premature shattering

of pods [5]. Despite the destructive nature of this pathogen, very little is known about the molecular determinants produced by *A. brassicae* except that it produces an array of phytotoxins including the well-characterized, host-selective toxin destruxin B [6].

Although resistance to *A. brassicae* has not been reported in any *Brassica* species, a high degree of tolerance to this pathogen has been reported in *Sinapis alba*, *Camelina sativa*, *Capsella bursa-pastoris* and *Eruca sativa* [7,8]. In many of these cases, resistance is mediated by the production of phytoalexins and, for example, the phytoalexin camelexin has been reported to have antifungal activity against *A. brassicae* and appeared to inhibit the production of destruxin B by *A. brassicae* [9]. Additionally, detoxification by plants of the phytotoxins produced by the fungus may also be crucial for mediating resistance to pathogen as previously observed in the case of *S. alba* where the toxin destruxin B is detoxified via hydroxylation and glycosylation [10,11].

Although extensive information on the phytotoxins produced by *A. brassicae* and the resistance in some plants

* Corresponding author. Tel.: +1 780 492 7584; fax: +1 780 492 4265.

E-mail address: nat@ualberta.ca (N.N.V. Kav).

¹ Present address: Crops Breeding Technologies International Inc., 3004-116 Street, Edmonton, Alberta T6J 3H9, Canada.

mediated by the detoxification of the phytotoxins or by the production of phytoalexins is available, to our knowledge, the molecular details accompanying pathogen infection has never been investigated in any host challenged with this pathogen. Investigating the changes in the transcriptome as well as the proteome that accompany a stress, such as pathogen challenge, can provide valuable information on the specific molecular responses that are occurring in response to the stress. In the post-genomic era, proteome analysis provides real insights into the molecular processes associated with environmental or developmental signals [12]. In fact, proteome analysis techniques including two-dimensional electrophoresis have been used extensively to investigate plant responses to various stresses including pathogen challenge [13–16]. Based on the proteome-level information obtained through these studies it may be possible to rationally select gene(s) that may have utility in improving plant productivity under conditions of stress [17,18].

As mentioned previously, resistance to *A. brassicae* has not been observed in any brassica species. However *B. carinata*, an amphidiploid member of the cruciferous family, exhibits a higher degree of tolerance to *A. brassicae* [19] and other diseases such as blackleg caused by *Leptosphaeria maculans* which affect canola crops [20,21]. Using *B. carinata* as a source of resistance genes, the University of Alberta canola breeding program has developed lines that exhibit increased resistance to blackleg [13], whereas the tolerance of these lines to *A. brassicae* has not been previously reported. We have now challenged the blackleg-resistant and -susceptible lines derived from the *B. napus* × *B. carinata* cross with *A. brassicae* and observed that the two lines differed in the degree of susceptibility/tolerance to *A. brassicae*. In addition, we have characterized the proteome-level changes in these two lines in response to *A. brassicae* and identified a number of proteins whose levels were significantly affected. Moreover, the expression of genes encoding three selected proteins, which were observed to be affected by the pathogen, was investigated at various time points following *A. brassicae*-challenge using quantitative real-time PCR (Q-RT-PCR). Our results provide some insights into the molecular basis underlying the differential responses of the two lines to this economically important plant pathogen and may be instrumental in the rational engineering of *B. napus* with increased tolerance.

2. Materials and methods

2.1. Plant and fungal material

A blackleg-resistant (02-17044-9) and -susceptible (02-17034-12) *B. napus* lines derived from an interspecific cross between *B. napus* and *B. carinata* and subsequent backcrosses with *B. napus* (BC₂F₆) have been previously described [13]. In this study, seeds from a doubled-haploid derivative of the blackleg-resistant line (03-11116; referred to as line 1) and from the blackleg-susceptible line (02-17034-12 referred to as line 2) were used to evaluate their susceptibility/tolerance to *A. brassicae*. An isolate of *A. brassicae* (UAMH 7476) was kindly

provided by Dr. J.P. Tewari, Department of Agricultural, Food and Nutritional Science at the University of Alberta and was used as a source of inoculum.

2.2. Plant inoculation

Seeds from both lines were germinated and grown in plastic inserts (7.5 cm × 5 cm; 2 seeds per insert) containing Metro Mix[®] 290 (Grace Horticultural Products, Ajax, Ontario, Canada) consisting of vermiculite and peat moss. Plants were grown in the greenhouse (22 °C day/18 °C night; 16 h photoperiod) for 2 weeks, fertilized once in 2 weeks with 200 ppm Peters[®] 20-20-20. The spore suspension of the pathogen was prepared by scraping mycelia and spores from plates of actively growing fungal cultures into water and filtering the suspension through four layers of cheesecloth to remove most of the mycelia. The filtered spore suspension was centrifuged at 2000 × *g* for 5 min and resuspended in deionized water. This centrifugation was repeated one more time in order to ensure a clear spore preparation free of metabolites. After the final wash, supernatant was discarded and spores were resuspended in water containing 0.05% Tween-20. The spores in this suspension were counted using a haemocytometer and the concentration was adjusted to 4 × 10⁵ spores/ml. This suspension was used to inoculate 2-week-old seedlings, which had been placed in a humidity chamber (100% RH) for 24 h. Inoculation was performed by gently wounding the true leaves (2 leaves/plant) with a pipette tip and placing 25 μl of spore suspension. For the uninoculated controls, 25 μl of sterile deionized water was used [13]. The plants were returned to the humidity chamber for 24 h after which they were placed in the greenhouse.

2.3. Disease evaluation

Disease evaluation was carried out 10 days post-inoculation on a total of 54 plants/treatment in three independent biological replicates (with at least 12 plants in each replicate). The numbers of diseased as well as tolerant plants were recorded, the percentage of disease incidence was calculated. For both lines disease severity was assessed using a scale described in Buchwaldt and Green [22] where a score of 0 indicates no symptoms; 1, symptoms detectable with light microscopy only; 2, small chlorotic areas and/or a few small necrotic spots; 3, larger chlorotic areas and/or larger necrotic spots; 4, severe chlorotic areas and/or many necrotic spots often coalescing; 5, larger areas with chlorosis and necrosis and often wilting of the tissue.

2.4. Harvest of plants and protein extraction for two-dimensional gel electrophoresis

Leaves (inoculated and newly formed) were collected from 10 plants for each treatment (12, 24, 48, 72 h post-inoculation) for proteome analysis, flash-frozen in liquid nitrogen and stored at –80 °C until use. Pooled leaf tissues from 10 plants (12, 24, 48 and 72 h post-inoculation with *A. brassicae* and control

plants) were ground to a fine powder using liquid nitrogen. Tissue powder (300 mg) was homogenized in 1 ml of acetone containing 10% (w/v) trichloroacetic acid (TCA) and 0.07% dithiothreitol (DTT). This extract was incubated at -20°C for 1 h, and centrifuged at $15,000 \times g$ for 15 min at 4°C , and the pellet was washed by resuspension in 1 ml of ice-cold acetone containing 0.07% DTT and centrifuged as described above. The pellet was washed four more times with ice-cold acetone containing 0.07% DTT, air-dried for 20 min and resuspended in 500 μl rehydration/sample buffer (Bio-Rad, Canada) containing 0.1% tributylphosphine (TBP) and incubated overnight at 4°C . The extracts were vortexed vigorously and centrifuged as above and the supernatants transferred to fresh tubes. The concentration of the protein in the supernatant was determined using a modified Bradford assay (Bio-Rad) and all samples were stored at -20°C until two-dimensional gel electrophoresis. Extracts from pooled leaf tissue were prepared from at least three independent inoculation experiments.

2.5. Two-dimensional electrophoresis

Isoelectric focusing (IEF) of protein extracts in the first-dimension as well as separation by SDS-PAGE in the second dimension was performed as previously described [13]. Briefly, 300 μg of protein in 300 μl of rehydration/sample buffer (8 M urea, 2% CHAPS, 40 mM DTT, 0.2% Bio-Lyte and 2 mM TBP) was used to passively hydrate 17 cm IPG strips (pI 4–7 linear; Bio-Rad). Isoelectric focusing was performed using a Bio-Rad PROTEAN IEF unit programmed to provide an optimum, maximum field strength of 600 V/cm and a 50 μA limit/IPG strip at 10,000 V for 60,000 V h. Prior to the focusing step, the strips were held at 250 V for 15 min to remove charged contaminants and at 500 V for 3 h after focusing to eliminate artifacts due to over- and under-focusing. Prior to second dimension SDS-PAGE, to solubilize focused proteins and allow SDS binding, the focused IPG strips were equilibrated in buffers containing SDS and DTT for the reduction of sulfhydryl groups followed by a second incubation in buffer containing iodoacetamide, which alkylates the reduced sulfhydryl groups. Second dimension electrophoresis was carried out on 13% polyacrylamide gels (20 cm \times 20 cm, 1 mm thickness) using a PROTEAN II xi system (Bio-Rad) at 45 V/gel until 2 h after the dye front reached the bottom of gel. Gels were stained with silver using Silver Stain Plus kit (Bio-Rad) and images of the stained gels were acquired using the GS-800 calibrated densitometer (Bio-Rad). For each time-point, images from at least three gels obtained from three independent inoculation experiments were compared.

2.6. Image analysis

Two-dimensional gels from the protein extracts of control and inoculated leaf tissue were analyzed using the PDQuest software (Bio-Rad). Gels from three independent biological replicates were used to make the match-sets and individual spots were matched (added or deleted) using software tools. Each set of gels from three replicates were analyzed simultaneously using

Student's *t*-test feature of this software in order to identify protein spots indicating statistically significant differences in levels as a result of pathogen challenge. Spot intensities of control and inoculated gels at different time points were determined using the spot quantification tool and the fold changes from controls were calculated. These spots were excised from the gels using a sterile scalpel and the proteins were identified using ESI-Q-ToF-MS/MS [13].

2.7. ESI-Q-ToF-MS/MS

Briefly, ESI-Q-ToF-MS/MS analysis for an excised protein sample was performed at the Institute for Biomolecular Design (IBD), University of Alberta, Canada. Processing of the gel pieces was performed in a fully automated fashion on a Mass Prep Station (Micromass, UK). The gel pieces were de-stained, reduced with 10 mM DTT, alkylated with 55 mM iodoacetamide and digested with 6 ng/ μl trypsin (Promega Sequencing Grade Modified) in 50 mM ammonium bicarbonate (25 μl) for 5 h at 37°C . The tryptic peptides were extracted after an enzymatic digestion and subjected to LC/MS/MS analysis on a Micromass Q-ToF-2 mass spectrometer (Micromass) coupled to a Waters CapLC capillary HPLC (Waters Corp., USA). This procedure involved separation on a PicoFrit 5 capillary reversed-phase column (5 μm BioBasic C18, 300 \AA pore size, 75 μm ID \times 10 cm, 15 μm tip, New Objectives, USA), using a linear water/acetonitrile gradient (0.2% Formic acid), with a 300 μm \times 5 mm PepMap C18 column (LC Packings, USA) being used as a loading/desalting column. The eluent was introduced directly to the mass spectrometer by electrospray ionization at the tip of the capillary column. Data dependent MS/MS acquisition was performed on detected peptides with a charge state of 2 or 3. Proteins were identified from the MS/MS data through a search of the NCBI non-redundant database using Mascot Daemon (Matrix Science, UK).

2.8. Q-RT-PCR

Primers for Q-RT-PCR were designed using the Primer Premier 3 software (Applied Biosystems Inc., USA) to generate PCR products of approximately 70–80 bp and are shown in Table 1. Total RNA was extracted from both plant lines using the QIAGEN RNeasy Plant Mini Kit (Qiagen, Canada) from pooled, leaf tissue obtained from control and pathogen challenged plants at various time points after infection and treated with RNase-free DNase (Qiagen). First strand cDNA was synthesized by reverse transcription of total RNA (50 ng) using the iScript cDNA synthesis kit (Bio-Rad, USA) and the subsequent PCR reaction was performed with 2 μl of 5 \times diluted cDNA as template, 22.5 pmol of the primers, 5 pmol of the probe and 1 \times TaqMan PCR Master Mix (Roche, USA) in a total volume of 20 μl . PCR analysis was performed using an ABI prism 7700 Sequence detector (Applied Biosystems) using the SNP RT template program and comparative relative expression of the various genes was determined using the delta-delta method employing the formula: relative expression = $2^{-[\Delta\text{Ct}_{\text{sample}} - \Delta\text{Ct}_{\text{control}}]}$ [23] where Ct refers to the threshold cycle, sample indicates the gene

Table 1
Primer sequences for quantitative real-time PCR analysis

Genes	Accession #	Primer pairs and probe used in real-time PCR
Germin-like protein	U21743	Forward; 5'-GGATTCATCTCCTCTGCCAACT-3' Reverse; 5'-CCATGACCTGTCCCGGTTT-3' Probe; 5'-TGTCTACGTGCAGACGC-3'
Peptidylprolyl <i>cis-trans</i> isomerase	M55018	Forward; 5'-CGGCAAATCCGGAAAGC-3' Reverse; 5'-GATCACGCGGTGGAAAGC-3' Probe; 5'-ACTCCACTACAAGGGC-3'
Auxin-induced protein	H07824	Forward; 5'-ACGAGACTTTTGGGAACATGGT-3' Reverse; 5'-TTGAGACGAAGACGATCTTTGC-3' Probe; 5'-CAGTCCGGTCGTGC-3'
Actin	AF111812	Forward; 5'-TGGGTTTGCTGGTGACGAT-3' Reverse; 5'-TGCCTAGGACGACCAACAATACT-3' Probe; 5'-CTCCCAGGGCTGTGTT-3'

of interest and control indicates the endogenous house-keeping gene. Level of expression in the uninoculated plants was equated to 1 and the relative expression in the inoculated plants was normalized against those levels. The reactions were performed in duplicate and the experiments were repeated at least three times and the results analyzed using Student's *t*-test.

3. Results and discussion

3.1. Response to *A. brassicae*

The two lines of *B. napus* were challenged with *A. brassicae* as described earlier and the effects of the pathogen on these two lines were evaluated. The appearance of the two *B. napus* lines used in the current study 10 days after challenge with *A. brassicae* is shown in Fig. 1. Line 1 exhibited severe chlorosis and necrosis that spread from the spot that had been inoculated with *A. brassicae* spores, had irregular margins extending towards the

periphery of the leaf suggesting that it was quite susceptible to *A. brassicae* (Fig. 1A and B). In contrast, the leaves of line 2 exhibited localized chlorosis and necrosis only around the inoculated region which clearly indicated that this line was more tolerant to the pathogen than its sister line (Fig. 1C and D). The average disease incidence was calculated as $9.13 \pm 0.50\%$ in the *Alternaria*-tolerant line (line 2) and $90.5 \pm 5.91\%$ in *Alternaria*-susceptible line (line 1) 10 days after inoculation with the pathogen. Lesions formed on line 1 were generally rated as "4" (severe chlorotic and/or necrotic spots, often coalescing) whereas lesions on line 2 were generally rated as "2" (smaller chlorotic and/or necrotic spots) [22]. These results suggest that line 2 is more tolerant of the two sister lines to *A. brassicae*.

3.2. Effect of pathogen on leaf proteomes

The effects of pathogen infection on the leaf proteome of the two *B. napus* lines were investigated at 12, 24, 48 and 72 h after

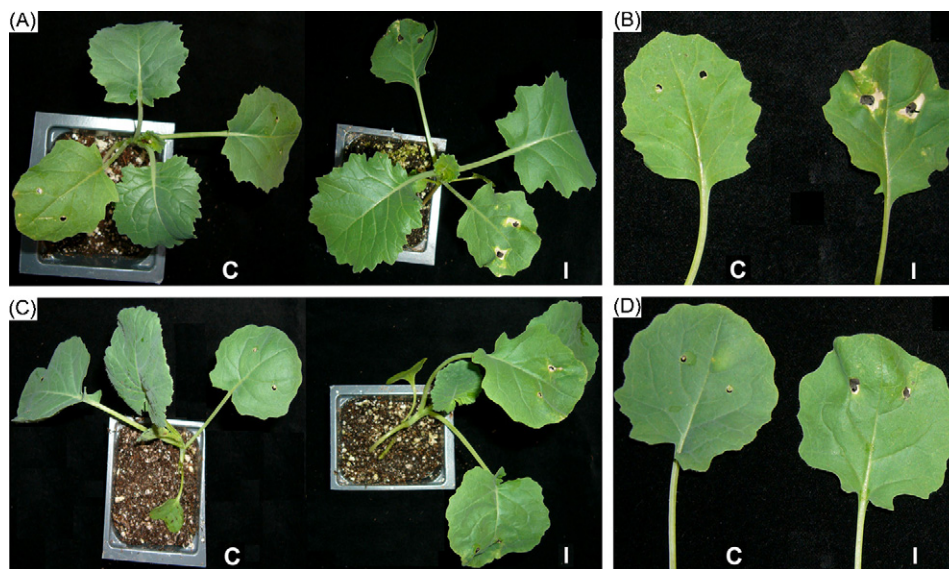


Fig. 1. Appearance of *Brassica napus* plants and leaves 10 days after challenge with *Alternaria brassicae*. Panels (A) and (C) show the chlorotic and necrotic lesions induced by the pathogen in the susceptible (line 1) and tolerant (line 2) lines, respectively while (B) and (D) are closer views of the challenged leaves from plants shown in (A) and (C). In all the panels the letter 'C' refers to control and 'I' to pathogen challenged plants.

inoculation using two-dimensional electrophoresis and representative images are shown in Figs. 2–11. Three independent gels (one from each of the three biological replicates) were analyzed for each treatment (control plants and pathogen challenged) using the Student's *t*-test and a total of 48 spots were observed to be reproducibly and significantly ($P < 0.05$) altered in intensities in the *Alternaria*-tolerant line (line 2). Representative proteome maps for the uninoculated controls and inoculated plants at various times after pathogen challenge for the *Alternaria*-tolerant line are shown in Figs. 2–5 and the arrows and numbers refer to spots exhibiting significant changes in spot volume after pathogen challenge. Among them, 4 spots were observed at 12, 9 at 24, 20 at 48 and 15 at 72 h post-inoculation (Fig. 6). Notably, the levels of 41 spots were observed to increase in intensity while the others exhibited a decrease (Fig. 6).

In the case of the line susceptible to *A. brassicae* (line 1), we observed a total of 23 spots to be altered in intensity (Figs. 7–11) in response to the pathogen, with 3 at 12, 7 at 24, 11 at 48 and 2 at 72 h post-inoculation with the pathogen (Fig. 11).

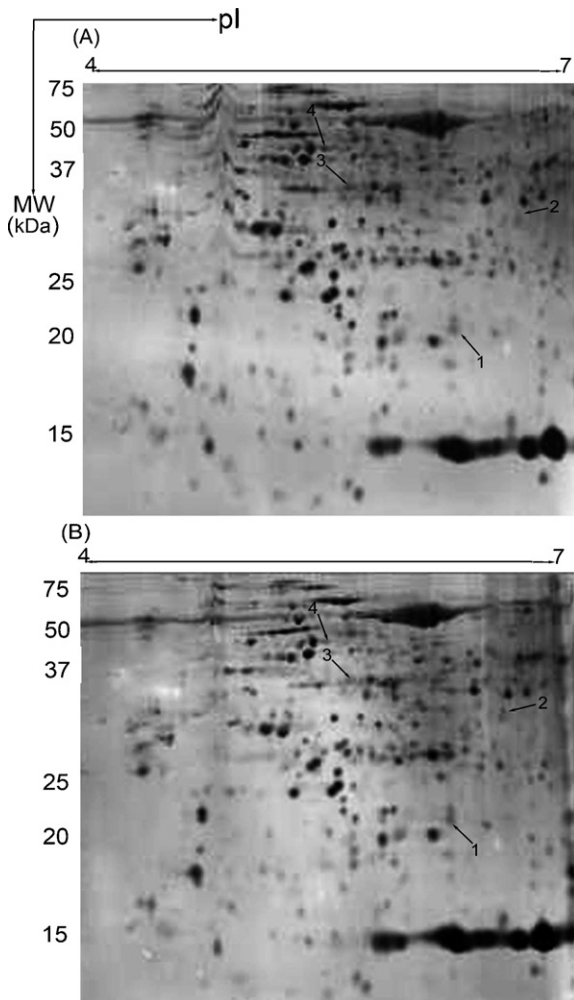


Fig. 2. Silver-stained images of two-dimensional gels of leaf protein extracted from the tolerant *B. napus* line 12 h after challenge with *A. brassicae*. Gels from control (A) and pathogen-challenged (B) leaf protein extracts are shown where arrows and numbers represent those protein spots whose intensities showed significant changes upon pathogen challenge.

In this case, the intensity of only 4 spots was observed to be increased whereas 19 spots decreased in intensity in response to the pathogen (Fig. 11). All these protein spots were excised from the gels and subjected to tandem mass spectrometry in order to establish their identities.

3.3. Identities of differentially expressed proteins upon pathogen infection

The identities of the proteins determined by ESI-Q-ToF-MS/MS, which bases its results on peptide mass fingerprints, are shown in Table 2. Using this technique, we were able to identify a total of 38 proteins (out of a total of 71 that were analyzed from the two lines), a success rate of ~53%, which is normal for this type of analysis. Three proteins were identified at 12, 6 after 24, 11 after 48 and 10 after 72 h after challenge with *A. brassicae* in the *Alternaria*-tolerant line (line 2) whereas, in the *Alternaria*-susceptible line (line 1) only 1 spot after 12, 2 after 24, 5 after 48 and 0 after 72 h of challenge were successfully identified. The identities of the

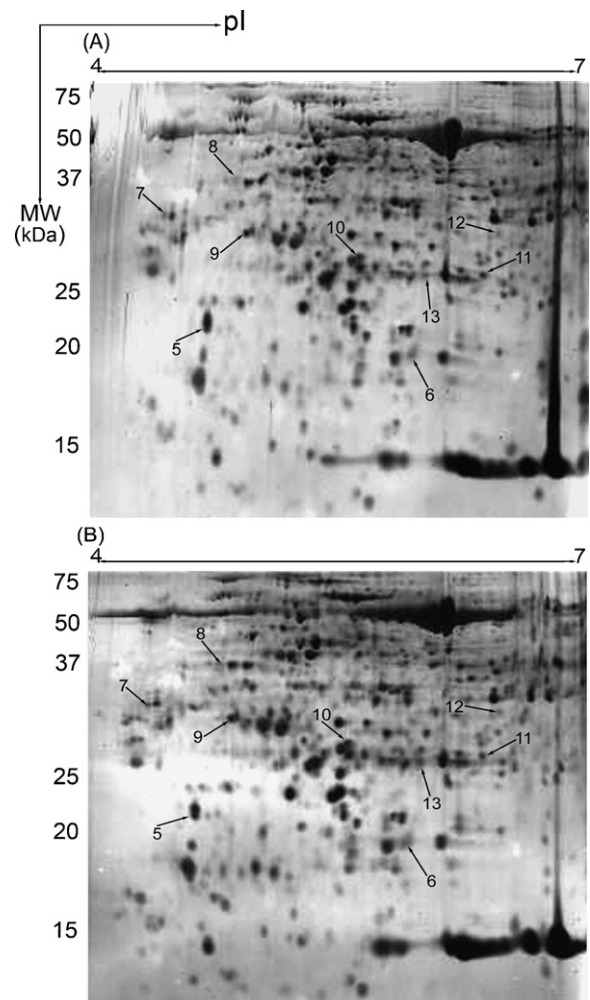


Fig. 3. Silver-stained images of two-dimensional gels of leaf protein extracted from the tolerant *B. napus* line 24 h after challenge with *A. brassicae*. Gels from control (A) and pathogen-challenged (B) leaf protein extracts are shown where arrows and numbers represent those protein spots whose intensities showed significant changes upon pathogen challenge.

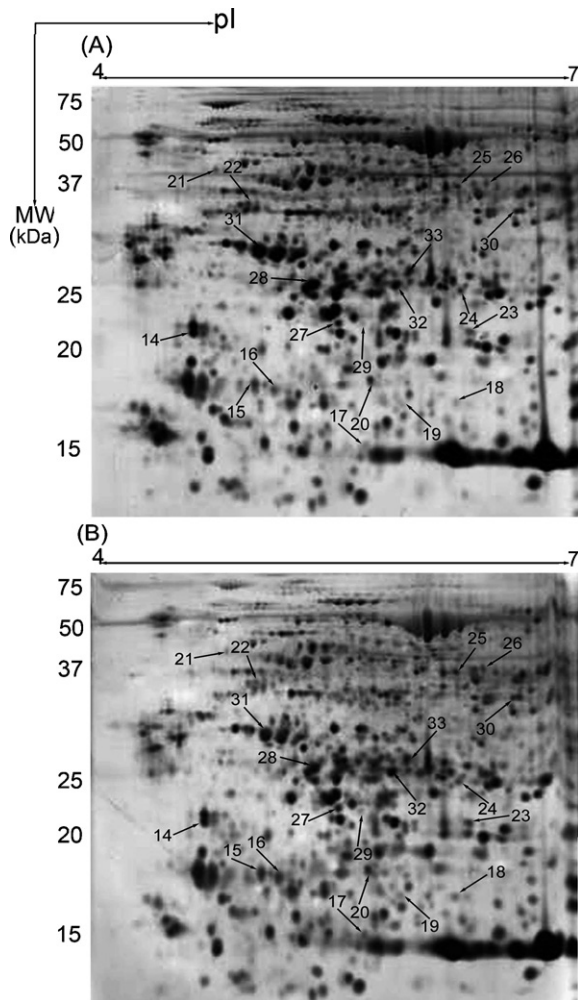


Fig. 4. Silver-stained images of two-dimensional gels of leaf protein extracted from the tolerant *B. napus* line 48 h after challenge with *A. brassicae*. Gels from control (A) and pathogen-challenged (B) leaf protein extracts are shown where arrows and numbers represent those protein spots whose intensities showed significant changes upon pathogen challenge.

proteins established by MS from these two lines are presented in Table 2 and were “significant hits” based on individual peptide ion scores. The ion score is automatically calculated by the Mascot program and is $-10 \times \log(P)$ where P is the probability that the observed match is a random event. When the ion scores exceed the threshold value for a random event, it indicates sequence identity or extensive homology ($P < 0.05$). Normally the identity of the spot is established as the protein that produced the highest score and, consequently, the best match with its peptide sequence.

A number of proteins involved in metabolic pathways, stabilization of protein structure and function, production and detoxification of reactive oxygen species (ROS), and signal transduction were identified as being affected in the tolerant line as a result of pathogen challenge (Table 2). Among them, those involved in the production and detoxification of ROS and signal transduction as well as specific metabolic pathways may have a direct bearing on the responses of the plant to the pathogen and are discussed in greater detail. In the case of the susceptible line, most of the proteins that were identified are

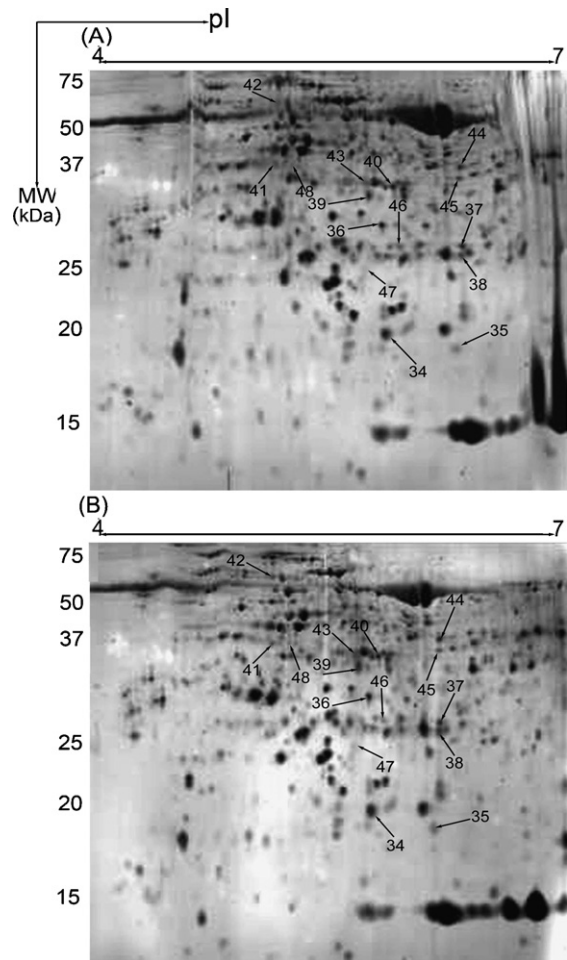


Fig. 5. Silver-stained images of two-dimensional gels of leaf protein extracted from the tolerant *B. napus* line 72 h after challenge with *A. brassicae*. Gels from control (A) and pathogen-challenged (B) leaf protein extracts are shown where arrows and numbers represent those protein spots whose intensities showed significant changes upon pathogen challenge.

involved in primary metabolic pathways with some exceptions (Table 2).

3.4. Proteins involved in metabolic pathways

A number of proteins that were identified in this study as being affected at various times after challenge with the pathogen are those associated with primary metabolic pathways. These include the large subunit of ribulose 1,5-bisphosphate carboxylase/oxygenase (Spot #2; Fig. 6; Table 2), aldolase (Spot #3; Fig. 6; Table 2), sedoheptulose bisphosphatase (Spots #8 and 12; Fig. 6; Table 2), triosephosphate isomerase (Spots #11, 37 and 46; Fig. 6; Table 2), chloroplastic malate dehydrogenase (Spot #30; Fig. 6; Table 2), putative enoyl-CoA hydratase (Spot #38; Fig. 6; Table 2) and cysteine synthase (Spot #39; Fig. 6; Table 2). The intensities of all the above-mentioned enzymes involved in primary metabolic pathways with the exception of aldolase (Spot #3; Fig. 6; Table 2) were found to be increased in the *Alternaria*-tolerant line (line 2). In addition, an inorganic pyrophosphatase-like

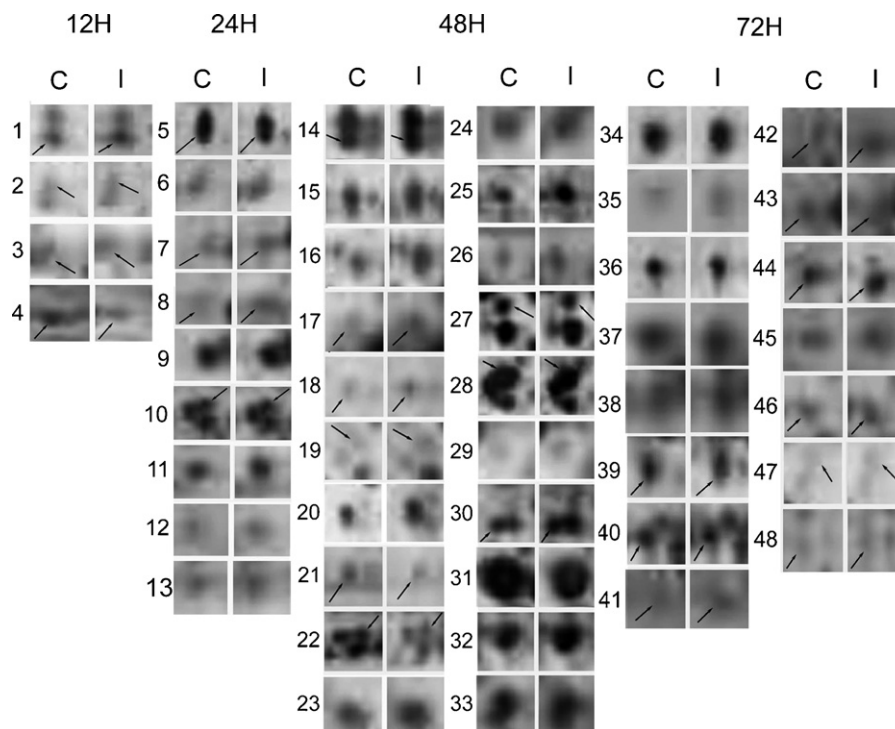


Fig. 6. A closer view of all the individual spots affected by pathogen challenge at various time points in the *Alternaria*-tolerant line. The spots from control (C) and pathogen challenged (I) are shown.

protein (Spot #9; Fig. 6; Table 2) and a protein associated with the oxygen-evolving complex of photosystem II (Spot #31; Fig. 6; Table 2), were also identified in this line with the intensity of the former increasing and that of the latter decreasing following pathogen challenge. In the *Alternaria*-susceptible line (line 1), as stated earlier, we observed that the intensities of all proteins with the exception of one (Spot #51; Fig. 11; Table 2) decreased. Because most of the proteins identified in this study were from the tolerant line, we have limited our discussion to those that we believe may play an important role in mediating the observed tolerance to the pathogen.

Our study identified the enzyme carbonic anhydrase (CA; Spot #36; Fig. 6; Table 2) in the *Alternaria*-tolerant line as being elevated 72 h after challenge with the pathogen and may have a direct role in combating the pathogen. CA has potential involvement in photosynthetic acclimation [24] and the requirement for the enzyme varies significantly among photosynthetic organisms. The role of CA in photosynthetic CO₂ fixation is to facilitate the supply of CO₂ to the sites of carboxylation within the chloroplasts. The increase in chloroplastic carbonic anhydrase appeared to be accompanied by a concomitant increase in Rubisco activity [25]. In addition, it has been reported that tobacco chloroplast CA also exhibited salicylic acid (SA)-binding activity [26]. Furthermore, the silencing of CA gene expression in leaves of *Nicotiana benthamiana* suppressed the *Pto:avrPto*-mediated hypersensitive reaction (HR) indicating that CA has a role in plant defense [26]. It is possible that the increase in CA may contribute to the increased tolerance of this *B. napus* line to *A.*

brassicae. Furthermore, the intensity of a spot identified as CA (Spot #64; Fig. 11; Table 2) was observed to decrease in the pathogen-challenged, *Alternaria*-susceptible line further supporting the possible involvement of CA in mediating tolerance to this fungal pathogen.

Another enzyme involved in plant metabolic pathways that may play a role in increasing the tolerance of this line (line 2) to *A. brassicae* is cinnamyl alcohol dehydrogenase (CAD; Spot #26; Fig. 6; Table 2), which was observed to be increased 48 h after pathogen challenge. CAD catalyzes the final step in phenylpropanoid synthesis specific to the production of lignin monomers [27]. Besides imparting mechanical rigidity, lignin is resistant to microbial degradation and provides an effective barrier to the invading pathogen. Lignification of infected tissue prevents further colonization of the invading pathogen, in effect isolating the fungus, and preventing the spread of the disease. For example, the induction of CAD in bean cell suspension cultures after treatment with fungal elicitor prepared from the mycelial cell wall of the pathogen *Colletotrichum lindemuthianum* has been previously reported [27,28]. Similarly, our proteome-based analysis indicates that enhanced lignin biosynthesis might play a role in mediating the observed effects during this host–pathogen interaction and should be investigated further.

3.5. Proteins involved in the production of reactive oxygen species (ROS)

Overproduction of ROS constitutes one of the first responses of plant cells to infection. In addition ROS can also contribute

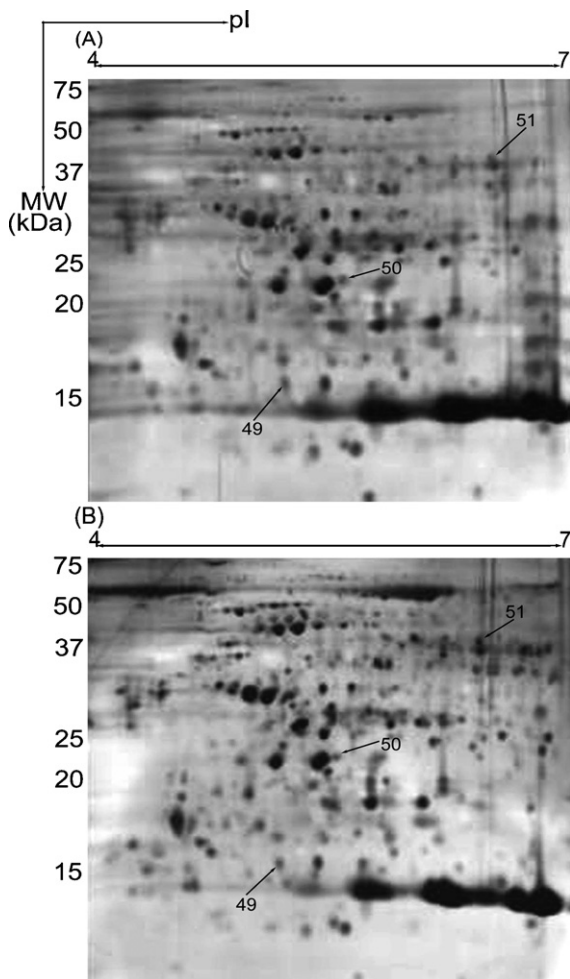


Fig. 7. Silver-stained images of two-dimensional gels of leaf protein extracted from the susceptible *B. napus* line 12 h after challenge with *A. brassicae*. Gels from control (A) and pathogen-challenged (B) leaf protein extracts are shown where arrows and numbers represent those protein spots whose intensities showed significant changes upon pathogen challenge.

to the programmed cell death (PCD), thereby serving as signal molecules for induction of local and systemic resistance [29]. The antioxidant enzymes identified in this study included a germin-like protein in the *Alternaria*-tolerant line (GLP; Spot #1; Fig. 6; Table 2) observed to be elevated at 12 h after infection. GLPs are functionally diverse proteins that belong to the cupin superfamily and are present in archaea, eubacteria and eukaryota, and are encoded by diverse multigene families in plants [30]. It has been proposed that germins and GLPs represent extracellular superoxide dismutases (SODs), involved in biotic and abiotic stress amelioration [31]. Furthermore, a SOD isolated from the moss *Barbula unguiculata* has been identified as a GLP [32]. The potential role of GLP in mediating the observed effects is supported by the fact that the expression of several barley germin and GLP genes has been found to be up-regulated during fungal infection of resistant plants [33]. Interestingly, our current study also identified a protein whose intensity was reduced in the *Alternaria*-susceptible line 24 h following pathogen challenge as a GLP (Spot #55; Fig. 11; Table 2), which suggests that the enhanced levels of GLP may

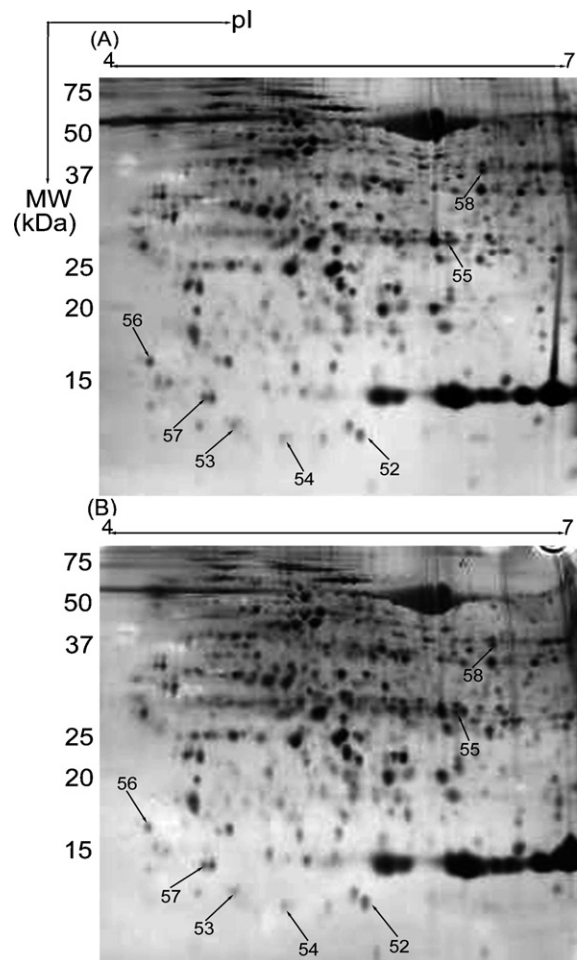


Fig. 8. Silver-stained images of two-dimensional gels of leaf protein extracted from the susceptible *B. napus* line 24 h after challenge with *A. brassicae*. Gels from control (A) and pathogen-challenged (B) leaf protein extracts are shown where arrows and numbers represent those protein spots whose intensities showed significant changes upon pathogen challenge.

have a significant role in mediating the observed responses to the pathogen in these two lines.

3.6. Proteins involved in detoxification of ROS

Several proteins involved in detoxifying free radicals generated during stress including pathogen challenge were identified as being elevated at 48 h after pathogen challenge in the *Alternaria*-tolerant line (line 2). These were peroxiredoxin (Spot #16; Fig. 6; Table 2), glutathione peroxidase (Spot #20; Fig. 6; Table 2) and a putative dehydroascorbate reductase (Spot #32; Fig. 6; Table 2). Components of ascorbate-glutathione cycle are widely distributed in the cellular compartments where ROS scavenging is required, indicating the importance of this cycle for maintaining the cellular ROS homeostasis. Elevated levels of glutathione peroxidase (GSH-Px) observed in this study may lead to amelioration of infection-induced oxidative stress [34]. Such a role is further supported by the fact that dehydroascorbate reductase is involved in the detoxification of H_2O_2 via the ascorbate-glutathione cycle and glutathione-dependent

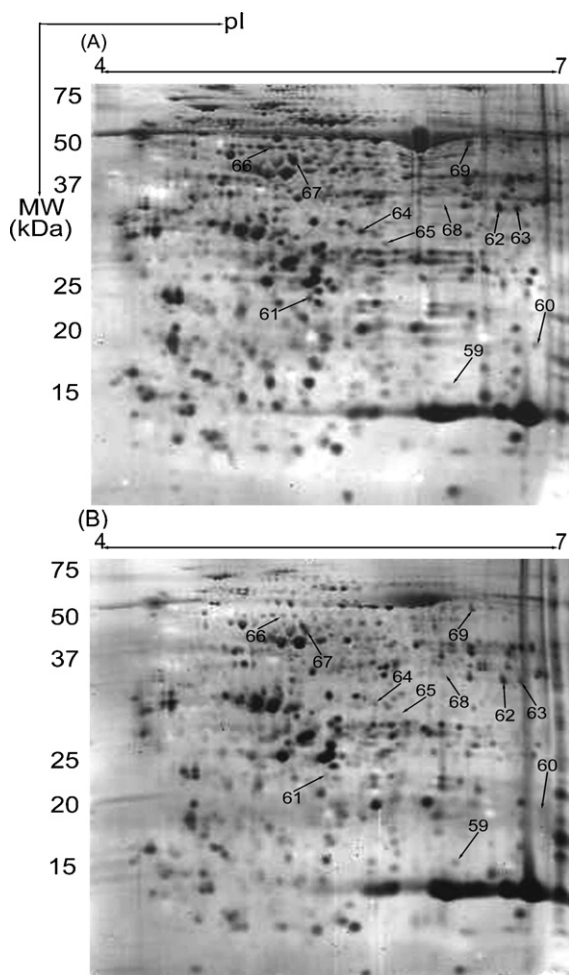


Fig. 9. Silver-stained images of two-dimensional gels of leaf protein extracted from the susceptible *B. napus* line 48 h after challenge with *A. brassicae*. Gels from control (A) and pathogen-challenged (B) leaf protein extracts are shown where arrows and numbers represent those protein spots whose intensities showed significant changes upon pathogen challenge.

peroxidase [35] and was identified in this study as being elevated in response to the pathogen. As mentioned earlier, another protein identified with established roles in the detoxification of ROS is a peroxiredoxin (Spot #16; Fig. 6; Table 2), which also detoxifies H_2O_2 and alkyl hydroperoxides using thioredoxins as electron donors [36]. Taken together, our observations suggest that the differences in the antioxidant responses, including GLP, peroxiredoxins, dehydroascorbate reductase and glutathione peroxidases may have an important role in mediating plant responses to *A. brassicae* challenge and, may play a key role in determining the outcome of the infection process.

3.7. ROS signal transduction

Another protein identified in this study as being increased in response to the pathogen in the *Alternaria*-tolerant line (line 2), showing >2-fold increase 48 h after challenge with the pathogen had similarities to nucleoside diphosphate kinase (NDPK) from *Arabidopsis thaliana* (Spot #19; Fig. 6; Table 2). NDPK is a house-keeping enzyme involved in

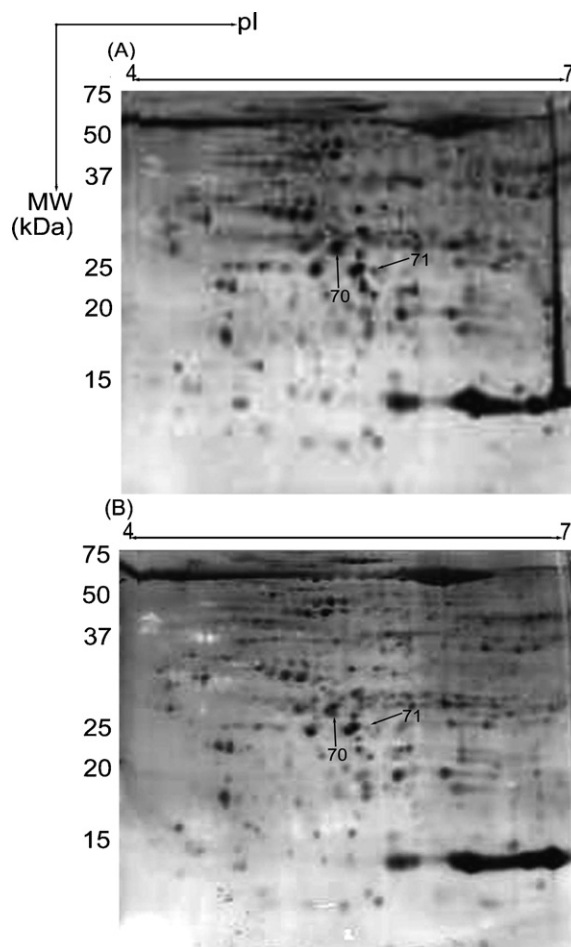


Fig. 10. Silver-stained images of two-dimensional gels of leaf protein extracted from the susceptible *B. napus* line 72 h after challenge with *A. brassicae*. Gels from control (A) and pathogen-challenged (B) leaf protein extracts are shown where arrows and numbers represent those protein spots whose intensities showed significant changes upon pathogen challenge.

maintaining cellular levels of all dNTPs (except ATP) and is known to play an important role in signal transduction pathways [37]. NDPK has been demonstrated to be involved in mediating abiotic stress as well as hormone responses in plants [38]. A direct connection between ROS that accumulates in response to pathogen challenge or abiotic stresses is supported by the observation that the constitutive expression of AtNDPK2 in *A. thaliana* reduced the accumulation of ROS and conferred multiple stress tolerance [39]. Furthermore, it was observed that this enhanced tolerance to abiotic stresses resulting from the expression of AtNDPK2 was mediated through the coordination of NDPK2 with MAPK-mediated H_2O_2 signaling. Our current observation that NDPK levels are increased in the tolerant line upon challenge with the pathogen, together with the elevated levels of enzymes detoxifying ROS suggest that ROS-mediated signaling involving NDPK might play an important role in mediating plant responses to *A. brassicae* challenge. A role for NDPK in mediating a response to this pathogen or, in the tolerance to this pathogen has not been previously reported and should be investigated further.

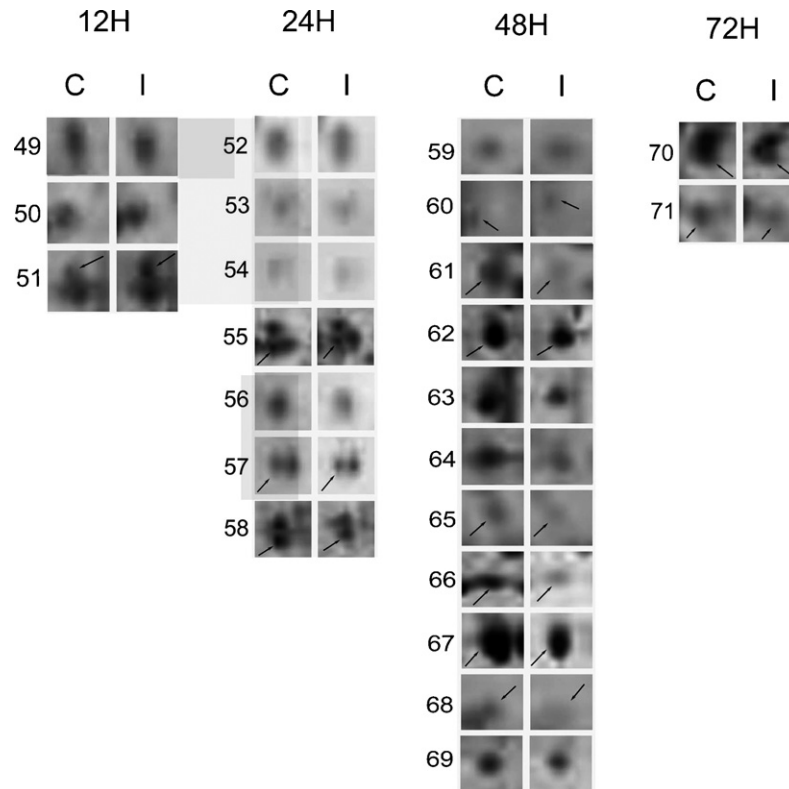


Fig. 11. A closer view of all the individual spots affected by pathogen challenge at various time points in the *Alternaria*-susceptible line. The spots from control (C) and pathogen challenged (I) are shown.

3.8. A role for auxin signaling?

Other proteins showing changes upon pathogen challenge in the *Alternaria*-tolerant line (line 2) included peptidylprolyl isomerase (PPIases; Spots #6 and 34; Fig. 6; Table 2), which showed modest but significant ($P < 0.05$) increases 24 and 72 h after pathogen challenge. PPIases, made up of the cyclophilins, the ubiquitous FK506-binding proteins and parvulins, catalyze the *cis*–*trans* isomerization of prolyl peptide bonds, a rate-limiting step in the folding of newly synthesized proteins [40]. Plant PPIase genes, in particular the cyclophilin genes, have been shown to be induced by a variety of biotic and abiotic stresses suggesting a role in mediating plant responses to stresses [41–43]. CYP20-3 (previously known as ROC4), identified in this study as showing increased expression at 24 and 72 h, is one of the highly conserved chloroplast cyclophilins [44]. Within the context of plant–pathogen interaction, elevated levels of PPIases have also been revealed by proteome analysis of germinating maize embryos in response to the pathogen *Fusarium verticillioides* [41]. Similarly, Godoy et al. [42] have reported the expression of a potato cyclophilin gene in response to *F. solani* infection. Our current observations suggest that PPIases may play an important role in this *A. brassicae*–*B. napus* pathosystem as well.

PPIases have also been implicated in auxin-mediated signal transduction [14,45]. The interaction of auxin with its cellular receptors triggers a cascade of events leading to the activation of other cellular processes resulting in responses including proton efflux from cells [46]. One of the effects of auxin is the modification of cell wall components such as lipids and altering

the orientation of cell wall polysaccharides [46]. Some genes involved in mediating cellular response to auxin are known to be involved in the regulation of an ubiquitin-dependent protein degradation process [47] and belong to the AUX/IAA protein family [48,49]. All the proteins in the AUX/IAA family have two highly conserved proline residues and the conformation (*cis* versus *trans*) of the prolyl peptide bonds are thought to be important for auxin-induced degradation of AUX/IAA proteins via the ubiquitin-dependent pathway [45,50]. Our observation that PPIase levels are increased as a result of challenge with the pathogen in the *B. napus* line suggests a potential role for auxin-mediated signaling during the host–pathogen interaction. Although this suggestion needs to be verified, we identified another protein spot whose levels were increased at 72 h after pathogen challenge in the *Alternaria*-tolerant line as an auxin-induced protein (Spot #40; Fig. 6; Table 2). Furthermore, a subunit of the multicatalytic endopeptidase complex proteasome precursor (Spot #47; Fig. 6; Table 2) was also observed to be elevated at 72 h in the present study in the *Alternaria*-tolerant line. As discussed above, the degradation of auxin responsive proteins via the proteasome degradation pathway is an important part of the auxin signaling process [51] and may be important in mediating tolerance to diseases as well [52].

Based on the increase in intensities of spots identified as NDPK, PPIase, auxin-responsive protein and the proteasome subunit, it is possible that auxin-mediated ROS signaling may be involved in mediating the higher tolerance of this *B. napus* line to *A. brassicae* perhaps by initiating programmed cell death (PCD) around the point of infection and preventing further

Table 2
 Details of proteins identified from *A. brassicae*-tolerant and -susceptible lines at various times after challenge with the pathogen

Spot #	Figure #	Hours post-inoculation (h)	Name of the protein	MS/MS ESI-Q-ToF			Accession # ^a	Mr/pI ^b	Status ^c
				PM (%) ^d	Score ^e	Sequence ^f			
Tolerant line									
1	2	12	Germin-like protein [<i>Arabidopsis thaliana</i>]	5	61	GPQSPSGYSCK	gi 1755184	22022/6.81	1.2 ± 0.06 ↑
2	2	12	Ribulose 1,5-bisphosphate carboxylase large subunit [<i>Vigna unguiculata</i>]	8	124	LNYYTPEYETK DTDILAAFR DDENVNSQPFMR SQAETGEIK	gi 3114999	52925/6.23	1.6 ± 0.12 ↑
3	2	12	Plastidic aldolase NPALDP1 [<i>Nicotiana paniculata</i>]	7	177	ALQNTCLK ASSYADELVK YTGEGESEEA	gi 4827251	42832/6.92	2.1 ± 0.31 ↓
6	3	24	Peptidylprolyl isomerase ROC4 [<i>A. thaliana</i>]	10	60	TLESQETR FEDENFTLK IYACGELPLDA	gi 6899901	28520/8.83	1.5 ± 0.23 ↑
7	3	24	eEF-1beta [<i>A. thaliana</i>]	8	36	SYITGYQASK LVPVGYGIK	gi 398606	25193/4.53	1.5 ± 0.00 ↑
8	3	24	Sedoheptulose-bisphosphatase precursor [<i>A. thaliana</i>]	2	62	ATFDNSEYSK	gi 22136118	42815/6.47	1.9 ± 0.29 ↑
9	3	24	Inorganic pyrophosphatase-like protein [<i>A. thaliana</i>]	3	64	IVAISLDDPK	gi 21592878	33658/5.55	1.4 ± 0.00 ↑
11	3	24	Triosephosphate isomerase [<i>A. thaliana</i>]	18	300	VAYALAQGLK EAGSTMDVVAQTK NVSADVAATTR IYGGSVNGGNCK	gi 7076787	27380/5.24	1.5 ± 0.23 ↑
12	3	24	Sedoheptulose-bisphosphatase precursor [<i>A. thaliana</i>]	2	62	ATFDNSEYSK	gi 7263568	42815/6.47	2.2 ± 0.89 ↑
16	4	48	Peroxiredoxin [<i>Hyacinthus orientalis</i>]	8	63	YALLAEDGVVK	gi 42565527	14120/5.43	4.4 ± 1.47 ↑
19	4	48	Nucleoside diphosphate kinase Ia [<i>A. thaliana</i>]	13	102	GDLAVQTGR TDPLQAEPGTIR	gi 3063661	17133/5.54	2.5 ± 0.79 ↑
20	4	48	Glutathione peroxidase [<i>Malus domestica</i>]	13	91	GNDVDLSTYK YAPTTSPLSIEK	gi 33308408	18690/6.14	1.6 ± 0.06 ↑
25	4	48	mRNA binding protein precursor-like [<i>A. thaliana</i>]	2.5	89	FSEIVSGGGK TNLPEDLKER DCEEWFFDR	gi 7573443	44074/8.54	2.0 ± 0.45 ↑
26	4	48	Cinnamyl alcohol dehydrogenase [<i>Brassica rapa</i>]	24	203	VTVISSPSK MVGGSIDIGMK LGADSFLVSSDPQK	gi 6683965	38948/6.9	1.6 ± 0.03 ↑
28	4	48	Chaperonin 10 [<i>A. thaliana</i>]	13	146	DGSNYIALR TAGGLLTETTK EDDIVGILETEDIK	gi 3057150	26913/8.86	1.3 ± 0.15 ↓

Table 2 (Continued)

Spot #	Figure #	Hours post-inoculation (h)	Name of the protein	MS/MS ESI-Q-ToF			Accession # ^a	Mr/pI ^b	Status ^c
				PM (%) ^d	Score ^e	Sequence ^f			
29	4	48	Chaperonin 10 [<i>A. thaliana</i>]	4	86	TAGLLLLTETTK	gi 3057150	26913/8.8	3.9 ± 1.68 ↑
30	4	48	Chloroplast NAD-MDH [<i>A. thaliana</i>]	2	86	IQNAGTEVVDAAK	gi 3256066	42623/8.48	1.6 ± 0.19 ↑
31	4	48	Putative protein 1 photosystem II oxygen-evolving complex [<i>A. thaliana</i>]	29	477	NAPPDFQNTK NTAASVGEITLK LTYDEIQSK VPFLFTVK FLVPSYR RLTYDEIQSK FCFEPTSFTVK GDEEELSKENVK QLDASGKPDNFTGK GGSTGYDNAVALPAGGR	gi 4835233	37078/6.78	1.4 ± 0.15 ↓
32	4	48	Putative dehydroascorbate reductase [<i>B. rapa</i>]	19	109	THDGPFIAGGK ALFSLDSFEK	gi 33285914	12029/6.15	1.3 ± 0.09 ↑
33	4	48	F18O14.33 [<i>A. thaliana</i>]	2	92	VSAVDLSLAPK	gi 8778432	50585/6.82	1.4 ± 0.12 ↑
34	5	72	Peptidylprolyl isomerase ROC4 [<i>A. thaliana</i>]	10	136	TLESQETR FEDENFTLK IYACGELPLDA	gi 6899901	28520/8.83	1.4 ± 0.13 ↑
36	5	72	Carbonic anhydrase [<i>Lycopersicon esculentum</i>]	6	59	YDTNPALYGELAK GGYYDFVK	gi 56562177	34845/6.67	2.2 ± 0.44 ↑
37	5	72	Triosephosphate isomerase [<i>A. thaliana</i>]	13	173	VAYALAQGLK EAGSTMDVVAAQTK NVSADVAATTR	gi 7076787	27380/5.24	1.5 ± 0.09 ↑
38	5	72	Putative enoyl-CoA hydratase [<i>Bradyrhizobium japonicum</i>]	2	51	EAI AETKR	gi 27381374	33104/5.53	3.2 ± 1.09 ↑
39	5	72	Cysteine synthase [<i>A. thaliana</i>]	9	129	LEIMEPCCSVK LILTMPASMSLER AFGAELVLTEPAK	gi 572517	41976/8.13	1.8 ± 0.12 ↑
40	5	72	Auxin-induced protein [<i>Vigna radiata</i>]	13	124	VVAAALNPVDAK EGDEVYANVSEK SLGADLAIDYTK GPFPSR	gi 4056456	32812/5.65	1.4 ± 0.03 ↑
44	5	72	mRNA binding protein precursor-like [<i>A. thaliana</i>]	2.5	108	FSEIVSGGGK TVEIVHYDPK TNLPEDLK	gi 7573443	44074/8.54	1.5 ± 0.03 ↑
45	5	72	Unnamed protein product [<i>Citrullus lanatus</i>]	3	83	TQDGGTEVVEAK	gi 18297	36406/8.8	1.3 ± 0.07 ↑
46	5	72	Triosephosphate isomerase 1 [<i>Zea mays</i>]	5	51	EAGSTMDVVAAQTK	gi 168647	27236/5.52	2.7 ± 1.46 ↑
47	5	72	Multicatalytic endopeptidase complex, proteasome precursor, beta subunit [<i>A. thaliana</i>]	4	52	TVIINSEGVTR	gi 21592365	24073/5.70	2.9 ± 0.74 ↑

Susceptible line									
51	6	12	mRNA binding protein [<i>A. thaliana</i>]	8	132	FSEIVSGGGK AVTLDGMAK TNLPEDLK FEEYVK	gi 15229384	44074/8.54	2.9 ± 1.0 ↑
55	7	24	Germin-like protein [<i>A. thaliana</i>]	5	71	GPQSPSGYSCK	gi 1755188	22020/6.81	3.1 ± 0.48 ↓
58	7	24	Putative malate dehydrogenase [<i>A. thaliana</i>]	10	158	SQAAALEK ALGQISER LSVPVSDVK MDLTAEELK	gi 21593602	35890/6.11	2.1 ± 0.50 ↓
62	8	48	Ferredoxin-NADP(+) reductase [<i>A. thaliana</i>]	4	181	EGQSVGVIADGIDK EQANDKGEK MYIQTR DNTFVYMCGLK	gi 15223753	41484/8.51	1.7 ± 0.13 ↓
63	8	48	Unnamed protein product [<i>C. lanatus</i>]	3	77	TQDGGTEVVEAK	gi 18297	36406/8.88	2.1 ± 0.40 ↓
64	8	48	Carbonic anhydrase [<i>L. esculentum</i>]	2	49	VDQITAEELK	gi 56562177	34845/6.67	2.7 ± 1.40 ↓
67	8	48	PGK1 phosphoglycerate kinase [<i>A. thaliana</i>]	11	315	SVGDLTSADLK ADLNVPLDDNQTITDDTR YLIENGAK AHASTEGVTK FAPDANSK	gi 15230595	50195/5.91	1.5 ± 0.02 ↓
69	8	48	Putative alanine aminotransferase [<i>A. thaliana</i>]	3	96	FCYNEK LMTDGFNSCK	gi 13430566	53776/6.91	1.3 ± 0.07 ↓

^a Accession numbers for the proteins generated by the Mascot search.

^b Theoretical molecular weight and *pI* values.

^c Fold increase in the intensity of a spot in the gels from pathogen-challenged tissue over the control gels. Average fold changes were calculated from at least three independent gels from three independent biological replicates (i.e. one gel from each replicate). Standard errors of the mean fold changes are also provided.

^d Percent sequence coverage.

^e Mascot score for the most significant hit calculated as described in Section 2.

^f Sequence of the peptide(s) that were matched based on the MS/MS fragmentation patterns.

spread of the lesion. Indeed, such a link between auxin and ROS has been described in a number of studies including one where the cytotoxic effects of indoleacetic acid (IAA) was demonstrated to be the result of increased levels of ROS [53]. In addition, the expression of a glutathione transferase/peroxidase gene (GST8) in *A. thaliana* has been shown to be induced by auxin [54]. Furthermore, the application of IAA reduced the disease incidence caused by the tomato pathogen *Fusarium oxysporum lycopersici* and increased plant-growth [55].

3.9. Analysis of gene expression using Q-RT-PCR

In order to further investigate whether the observed proteome changes are substantiated by changes in mRNA levels for those proteins involved in ROS-mediated auxin signaling, we investigated the expression of GLP, PPIase and auxin-induced protein. Q-RT-PCR analysis was performed using RNA isolated from leaves of unchallenged and *Alternaria*-challenged plants from both lines at 12, 24, 48 and 72 h after challenge. The results obtained are presented in Fig. 12 and the differential expression of these three genes in the tolerant line in response to the pathogen is evident. For example, GLP showed a modest increase in protein levels at 12 h after pathogen challenge in the *Alternaria*-tolerant line whereas it showed a significant decrease in intensity 24 h after pathogen challenge in the *Alternaria*-susceptible line. In the Q-RT-PCR experiments, we observed a nearly significant ($P < 0.06$) increase in GLP transcript at 24 h and a significant ($P < 0.05$) increase at 48 h after pathogen challenge in the *Alternaria*-tolerant line (Fig. 12A). Even though the increase in GLP protein (Table 2) as well as transcript levels (Fig. 12A) in the *Alternaria*-tolerant line may be modest, the decline of GLP protein level in the *Alternaria*-susceptible line is more dramatic (~3-fold; Table 2) but the transcript levels do not show such a dramatic decrease in this line following pathogen challenge (Fig. 12A). However, the decrease in GLP protein in the *Alternaria*-susceptible line may be important for the eventual outcome of the host–pathogen interaction, i.e. disease progression.

In the case of PPIase, we observed a significant ($P < 0.05$) increase in transcript levels at 12 h after pathogen challenge (Fig. 12B) whereas increase in protein levels was observed at 24 and 72 h (Table 2). Similar to PPIase, an apparent increase in the auxin-induced protein transcript was observed at 48 h (Fig. 12C) whereas a significant but modest increase in protein was observed at 72 h (Table 2). Our Q-RT-PCR results do not correlate well with the observed changes in protein levels for the auxin-induced protein and does not correlate with the specific time points where we observed changes in GLP and PPIase protein levels. However, the results from proteome analysis are probably more meaningful with respect to biological activities of the proteins.

4. Concluding remarks

Proteome analysis has the potential to provide significant insights into the molecular events that occur during plant–pathogen interactions. In this study, we have investigated the

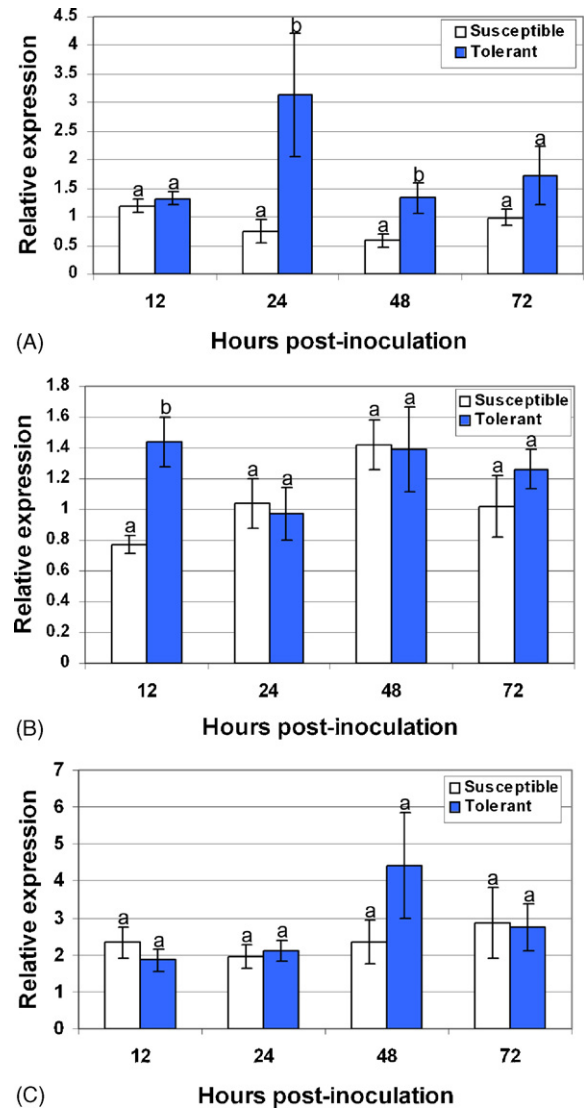


Fig. 12. Q-RT-PCR analysis of gene expression. The relative expression of germin-like protein (A), peptidylprolyl isomerase (B) and auxin-induced protein (C) at 12, 24, 48 and 72 h following inoculation with *A. brassicae* in the susceptible and tolerant lines of *B. napus* are shown. Bars with different letters indicate significant ($P < 0.05$) differences between the treatments.

proteome-level changes that occur during *A. brassicae*–*B. napus* interaction using two-dimensional electrophoresis and mass spectrometry. Such an investigation aimed at understanding these events in this pathosystem has not been previously reported. The identities of some of the proteins that showed pathogen-induced changes in quantity in these two lines pointed to specific biochemical processes that may be differentially altered at various time points following the pathogen challenge in these two lines. These include enzymes involved in the generation of ROS, their detoxification, signal transduction, as well as responses to the phytohormone auxin. However, the increase in levels of many of these proteins are quite modest and based on our proteome and Q-RT-PCR results reported here it may be premature to propose a definitive role for auxin and ROS signaling in mediating plant responses to this pathogen. Additional investigation into the expression of

various genes in ROS/auxin signaling pathway at earlier time points after pathogen challenge is warranted and may provide much needed information. Results from such studies may also open novel avenues for engineering durable resistance to this pathogen and are currently underway in our laboratory.

Acknowledgements

Financial support from Alberta Crop Industry Development Fund (ACIDF), Natural Sciences and Engineering Research Council of Canada (NSERC) and Alberta Agricultural Research Institute (AARI) is gratefully acknowledged. The assistance of Drs. Mike Ellison and Lorne Burke at the Institute for Biomolecular Design (IBD) with Mass Spectrometry and that of Mohsen Mohammadi with statistical analysis is also acknowledged.

References

- [1] P.R. Verma, G.S. Saharan, Monograph on Alternaria Diseases of Crucifers, Agriculture and Agri-Food Canada, Saskatoon, SK, Canada, 1994 p. 162.
- [2] G.S. Saharan, Disease resistance, in: K.S. Labana, S.S. Banga, S.K. Banga (Eds.), Breeding Oilseed Brassicas, Monographs on Theoretical and Applied Genetics, vol. 19, Springer, Berlin, Heidelberg, New York, 1993, pp. 181–205.
- [3] S.V. Rude, G.A. Petrie, E. Seidle, Effect of Alternaria blackspot on green seed content in canola (rapeseed), Can. J. Plant Pathol. 16 (1994) 252.
- [4] L.J. Duczek, E. Seidle, S.L. Reed, The effect of Alternaria blackspot on yield and seed quality of *Brassica rapa* in Saskatchewan, Can. J. Plant Pathol. 20 (1998) 217.
- [5] P.S. Bains, J.P. Tewari, Purification, chemical characterization and host-specificity of the toxin produced by *Alternaria brassicae*, Physiol. Mol. Plant Pathol. 30 (1987) 259–271.
- [6] M.S.C. Pedras, L.I. Zaharia, D. Ward, The destruxins: synthesis, biosynthesis, biotransformation and biological activity, Phytochemistry 59 (2002) 579–596.
- [7] K.L. Conn, J.P. Tewari, J.S. Dahiya, Resistance to *Alternaria brassicae* and phytoalexin-elicitation in rapeseed and other crucifers, Plant Sci. 56 (1988) 21–25.
- [8] K.L. Conn, J.P. Tewari, Hypersensitive reaction induced by *Alternaria brassicae* in *Eruca sativa*, an oil yielding crucifer, Can. J. Plant Pathol. 8 (1986) 348.
- [9] M.S.C. Pedras, A.Q. Khan, J.L. Taylor, The phytoalexin camalexin is not metabolized by *Phoma lingam*, *Alternaria brassicae*, or phytopathogenic bacteria, Plant Sci. 139 (1998) 1–8.
- [10] M.S.C. Pedras, I.L. Zaharia, Y. Gai, Y. Zhou, D.E. Ward, In planta sequential hydroxylation and glycosylation of a fungal phytotoxin: avoiding cell death and overcoming the fungal invader, Proc. Natl. Acad. Sci. U.S.A. 98 (2001) 747–752.
- [11] M.S.C. Pedras, S. Montaut, I.L. Zaharia, Y. Gai, D.E. Ward, Biotransformation of the host-selective toxin destruxin B by wild crucifers: probing a detoxification pathway, Phytochemistry 64 (2003) 957–963.
- [12] S.P. Gygi, R. Aebersold, Mass spectrometry and proteomics, Curr. Opin. Chem. Biol. 4 (2000) 489–494.
- [13] B. Subramanian, V.K. Bansal, N.N.V. Kav, Proteome-level investigation of *Brassica carinata*-derived resistance to *Leptosphaeria maculans*, J. Agric. Food Chem. 53 (2005) 313–324.
- [14] W. Yajima, J.C. Hall, N.N.V. Kav, Proteome-level differences between auxinic-herbicide-susceptible and -resistant wild mustard (*Sinapis arvensis* L.), J. Agric. Food Chem. 52 (2004) 5063–5070.
- [15] W. Zhou, F.L. Kolb, D.E. Riechers, Identification of proteins induced or upregulated by Fusarium head blight infection in the spikes of hexaploid wheat (*Triticum aestivum*), Genome 48 (2005) 770–780.
- [16] C. Rampitsch, N.V. Bykova, B. McCallum, E. Beimcik, W. Ens, Analysis of the wheat and *Puccinia triticina* (leaf rust) proteomes during a susceptible host–pathogen interaction, Proteomics 6 (2006) 1897–1907.
- [17] S. Srivastava, B. Fristensky, N.N.V. Kav, Constitutive expression of a PR10 protein enhances the germination of *Brassica napus* under saline conditions, Plant Cell Physiol. 45 (2004) 1320–1324.
- [18] S. Srivastava, M.H. Rahman, S. Shah, N.N.V. Kav, Constitutive expression of the pea ABA-responsive 17 (ABR17) cDNA confers multiple stress tolerance in *Arabidopsis thaliana*, Plant Biotech. J. 4 (2006) 529–549.
- [19] V.K. Bansal, G. Seguin-Swartz, G.F.W. Rakow, G.A. Petrie, Reaction of *Brassica* species to infection by *Alternaria brassicae*, Can. J. Plant Sci. 70 (1990) 1159–1162.
- [20] M.D. Sacristan, M. Gerdemann, Different behaviour of *Brassica juncea* and *Brassica carinata* as sources of *Phoma lingam* resistance in experiments of interspecific transfer to *Brassica napus*, Z. Pflanzenzuchtg. 97 (1986) 304–314.
- [21] S.R. Rimmer, C.G.J. van den Berg, Resistance of oil seed *Brassica* spp. to blackleg caused by *Leptosphaeria maculans*, Can. J. Plant Pathol. 14 (1992) 56–66.
- [22] L. Buchwaldt, H. Green, Phytotoxicity of destruxin B and its possible role in the pathogenesis of *Alternaria brassicae*, Plant Pathol. 41 (1992) 55–63.
- [23] K.J. Livak, T.D. Schmittgen, Analysis of relative gene expression data using real-time quantitative PCR and the 2- $\Delta\Delta C_t$ method, Methods 25 (2001) 402–408.
- [24] M.A. Porter, B. Grodzinski, Acclimation to high CO₂ in bean: carbonic anhydrase and ribulose biphosphate carboxylase, Plant Physiol. 74 (1984) 413–416.
- [25] N. Majeau, J.R. Coleman, Correlation of carbonic anhydrase and ribulose-1,5-biphosphate carboxylase/oxygenase expression in pea, Plant Physiol. 104 (1994) 1393–1399.
- [26] D.H. Slaymaker, D.A. Navarre, D. Clark, O. del Pozo, G.B. Martin, D.F. Klessig, The tobacco salicylic acid-binding protein 3 (SABP3) is the chloroplast carbonic anhydrase, which exhibits antioxidant activity and plays a role in the hypersensitive defense response, Proc. Natl. Acad. Sci. U.S.A. 99 (2002) 11640–11645.
- [27] M.H. Walter, J. Grima-Pettenat, C. Grand, A.M. Boudet, C.J. Lamb, Cinnamyl-alcohol dehydrogenase, a molecular marker specific for lignin synthesis: cDNA cloning and mRNA induction by fungal elicitor, Proc. Natl. Acad. Sci. U.S.A. 85 (1988) 5546–5550.
- [28] C. Grand, F. Sarni, C.J. Lamb, Rapid induction by fungal elicitor of the synthesis of cinnamyl-alcohol dehydrogenase, a specific enzyme of lignin synthesis, Eur. J. Biochem. 169 (1987) 73–77.
- [29] F.J. Corpas, J.B. Barroso, L.A. del Rio, Peroxisomes as a source of reactive oxygen species and nitric oxide signal molecules in plant cells, Trends Plant Sci. 6 (2001) 145–150.
- [30] J.M. Dunwell, S. Khuri, P.J. Gane, Microbial relatives of the seed storage proteins of higher plants: conservation of structure and diversification of function during evolution of the cupin superfamily, Microbiol. Mol. Biol. Rev. 64 (2000) 153–179.
- [31] E.J. Woo, M.J. Dumwell, P.W. Goodenough, A.C. Marvier, R.W. Pickersgill, Germin is a manganese containing homohexamer with oxalate oxidase and superoxide dismutase activities, Nat. Struct. Biol. 7 (2000) 1036–1040.
- [32] T. Yamahara, T. Shiono, T. Suzuki, K. Tanaka, S. Takio, K. Sato, S. Yamazaki, T. Satoh, Isolation of a germin-like protein with manganese superoxide dismutase activity from cells of a moss, *Barbula unguiculata*, J. Biol. Chem. 274 (1999) 33274–33278.
- [33] F. Zhou, Z. Zhang, P.L. Gregersen, J.D. Mikkelsen, E.D. Neergaard, D.B. Collinge, H.T. Christensen, Molecular characterization of the oxalate oxidase involved in the response of barley to the powdery mildew fungus, Plant Physiol. 117 (1998) 33–41.
- [34] D.P. Dixon, L. Cummins, D.J. Cole, R. Edwards, Glutathione-mediated detoxification systems in plants, Curr. Opin. Plant Biol. 1 (1998) 258–266.
- [35] L.A. del Rio, G.M. Pastori, J.M. Palma, L.M. Sandalio, F. Sevilla, F.J. Corpas, A. Jimenez, E. Lopez-Huertas, J.A. Hernandez, The activated oxygen role of peroxisomes in senescence, Plant Physiol. 116 (1998) 1195–1200.

- [36] L.B. Poole, A. Godzik, A. Nayeem, J.D. Schmitt, AhpF can be dissected into 2 functional units: tandem repeats of 2-thioredoxin-like folds in the terminus mediate electron transfer from the thioredoxin reductase like C-terminus to hpC, *Biochemistry* 39 (2000) 6602–6615.
- [37] A.S. Otero, NM23/nucleoside diphosphate kinase and signal transduction, *J. Bioenerg. Biomembr.* 32 (2000) 269–275.
- [38] M.L. Escobar Galvis, S. Marttila, G. Hakansson, J. Forsberg, C. Knorrp, Heat stress response in pea involves interaction of mitochondrial nucleoside diphosphate kinase with a novel 86-kilodalton protein, *Plant Physiol.* 126 (2001) 69–77.
- [39] H. Moon, B. Lee, G. Choi, D. Shin, D.T. Prasad, O. Lee, S.-S. Kwak, D.H. Kim, J. Nam, J. Bahk, J.C. Hong, S.Y. Lee, M.J. Cho, C.O. Lim, D.-J. Yun, NDP kinase 2 interacts with two oxidative stress activated MAPKs to regulate cellular redox state and enhances multiple stress tolerance in transgenic plants, *Proc. Natl. Acad. Sci. U.S.A.* 100 (2003) 358–363.
- [40] F.X. Schmid, Prolyl isomerases, *Adv. Protein Chem.* 59 (2001) 243–282.
- [41] S. Campo, M. Carrascal, M. Coca, J. Abian, S.S. Segundo, The defense response of germinating maize embryos against fungal infection: a proteomics approach, *Proteomics* 4 (2004) 383–396.
- [42] A.V. Godoy, A.S. Lazzaro, C.A. Casalongue, B.S. Segundo, Expression of a *Solanum tuberosum* cyclophilin gene is regulated by fungal infection and abiotic stress conditions, *Plant Sci.* 152 (2000) 123–134.
- [43] L. Andreeva, R. Heads, C.J. Green, Cyclophilins and their possible role in the stress response, *Int. J. Exp. Pathol.* 80 (1999) 305–315.
- [44] V. Lippuner, I.T. Chou, S.V. Scott, W.F. Ettinger, S.M. Theg, C.S. Gasser, Cloning and characterization of chloroplast and cytosolic forms of cyclophilin from *Arabidopsis thaliana*, *J. Biol. Chem.* 269 (1994) 7863–7868.
- [45] N. Dharmasiri, S. Dharmasiri, A.M. Jones, M. Estelle, Auxin action in a cell free system, *Curr. Biol.* 13 (2003) 1418–1422.
- [46] H. Macdonald, Auxin perception and signal transduction, *Physiol. Plant.* 100 (1997) 423–430.
- [47] O. Leyser, Molecular genetics of auxin signaling, *Annu. Rev. Plant Biol.* 53 (2002) 377–398.
- [48] P. Nagpal, L.M. Walker, J.C. Young, A. Sonawala, C. Timpte, M. Estelle, J.W. Reed, AXR2 encodes a member of the Aux/IAA protein family, *Plant Physiol.* 123 (2000) 563–573.
- [49] D. Rouse, P. Mackay, P. Stirnberg, M. Estelle, O. Leyser, Changes in auxin response from mutations in an Aux/IAA gene, *Science* 279 (1998) 1371–1373.
- [50] S.B. Tiwari, X.J. Wang, G. Hagen, T.J. Guilfoyle, Aux/IAA proteins are active repressors and their stability and activity are modulated by auxin, *Plant Cell* 13 (2001) 2809–2822.
- [51] N. Dharmasiri, M. Estelle, Auxin signaling and regulated protein degradation, *Trends Plant Sci.* 6 (2004) 302–308.
- [52] W.M. Gray, P.R. Muskett, H.W. Chuang, J.E. Parker, Arabidopsis SGT1b is required for SCF(TIR1)-mediated auxin response, *Plant Cell* 15 (2003) 1310–1319.
- [53] M.P. de Melo, T.M. de Lima, T.C. Pithon-Curi, R. Curi, The mechanism of indoleacetic acid cytotoxicity, *Toxicol. Lett.* 148 (2004) 103–111.
- [54] M.W. Bianchi, C. Roux, N. Vartanian, Drought regulation of GST8, encoding the Arabidopsis homologue of ParC/Nt107 glutathione transferase/peroxidase, *Physiol. Plant.* 116 (2002) 96–105.
- [55] E.F. Sharaf, A.A. Farrag, Induced resistance in tomato plants by IAA against *Fusarium oxysporum lycopersici*, *Pol. J. Microbiol.* 53 (2004) 111–116.